



## Critical error fields for locked mode instability in tokamaks

R. J. La Haye, R. Fitzpatrick, T. C. Hender, A. W. Morris, J. T. Scoville, and T. N. Todd

Citation: *Physics of Fluids B: Plasma Physics (1989-1993)* **4**, 2098 (1992); doi: 10.1063/1.860017

View online: <http://dx.doi.org/10.1063/1.860017>

View Table of Contents: <http://scitation.aip.org/content/aip/journal/pofb/4/7?ver=pdfcov>

Published by the [AIP Publishing](#)

---

### Articles you may be interested in

[Poloidal rotation in tokamaks with large electric field gradients](#)

*Phys. Plasmas* **2**, 159 (1995); 10.1063/1.871105

[Diocotron instability in curved magnetic field](#)

*Phys. Fluids B* **5**, 2334 (1993); 10.1063/1.860768

[Edge poloidal rotation profiles of H-mode plasmas in the JFT-2M tokamak](#)

*Phys. Fluids B* **4**, 2552 (1992); 10.1063/1.860486

[Two-dimensional numerical simulation of trapped electron mode turbulent transport in a tokamak](#)

*Phys. Fluids B* **3**, 3539 (1991); 10.1063/1.859734

[Tokamak error fields and locked modes](#)

*Phys. Fluids B* **3**, 2230 (1991); 10.1063/1.859640

---

# Critical error fields for locked mode instability in tokamaks\*

R. J. La Haye,<sup>†</sup> R. Fitzpatrick,<sup>a)</sup> T. C. Hender,<sup>a)</sup> A. W. Morris,<sup>a)</sup> J. T. Scoville,  
and T. N. Todd<sup>a)</sup>

General Atomics, San Diego, California 92138

(Received 18 November 1991; accepted 26 February 1992)

Otherwise stable discharges can become nonlinearly unstable to disruptive locked modes when subjected to a resonant  $m=2$ ,  $n=1$  error field from irregular poloidal field coils, as in DIII-D [Nucl. Fusion **31**, 875 (1991)], or from resonant magnetic perturbation coils as in COMPASS-C [Proceedings of the 18th European Conference on Controlled Fusion and Plasma Physics, Berlin (EPS, Petit-Lancy, Switzerland, 1991), Vol. 15C, Part II, p. 61]. Experiments in Ohmically heated deuterium discharges with  $q \approx 3.5$ ,  $\bar{n} \approx 2 \times 10^{19} \text{ m}^{-3}$  and  $B_T \approx 1.2 \text{ T}$  show that a much larger relative error field ( $B_{r21}/B_T \approx 1 \times 10^{-3}$ ) is required to produce a locked mode in the small, rapidly rotating plasma of COMPASS-C ( $R_0 = 0.56 \text{ m}$ ,  $f \approx 13 \text{ kHz}$ ) than in the medium-sized plasmas of DIII-D ( $R_0 = 1.67 \text{ m}$ ,  $f \approx 1.6 \text{ kHz}$ ), where the critical relative error field is  $B_{r21}/B_T \approx 2 \times 10^{-4}$ . This dependence of the threshold for instability is explained by a nonlinear tearing theory of the interaction of resonant magnetic perturbations with rotating plasmas that predicts the critical error field scales as  $(fR_0/B_T)^{4/3} \bar{n}^{2/3}$ . Extrapolating from existing devices, the predicted critical field for locked modes in Ohmic discharges on the International Thermonuclear Experimental Reactor (ITER) [Nucl. Fusion **30**, 1183 (1990)] ( $f=0.17 \text{ kHz}$ ,  $R_0 = 6.0 \text{ m}$ ,  $B_T = 4.9 \text{ T}$ ,  $\bar{n} = 2 \times 10^{19} \text{ m}^{-3}$ ) is  $B_{r21}/B_T \approx 2 \times 10^{-5}$ . Such error fields could be produced by shifts and/or tilts of only one of the larger poloidal field coils of as little as 0.6 cm with respect to the toroidal field. A means to increase the rotation frequency would obviate the sensitivity to error fields and increase allowable tolerances on coil construction.

## I. INTRODUCTION

Locked modes are observed in many tokamaks.<sup>1-6</sup> The locked mode is typically a nearly purely growing, nonrotating, nonaxisymmetric magnetic field perturbation with poloidal mode number  $m \approx 2$  and toroidal mode number  $n=1$ . Rotating modes are sometimes observed to slow down and lock while locked modes with no rotating precursor are also observed. Because of the mode's low frequency, detection requires combinations of magnetic loops whose signals are integrated and distinguished from the background axisymmetric  $n=0$  magnetic field. When mode rotation completely ceases, the locking occurs with the  $n=1$  radial field aligned at the same toroidal location in phase with the external applied or intrinsic static error field.<sup>1</sup>

Characteristics of discharges with locked modes include reduced energy confinement, cessation of soft x-ray (SXR) sawteeth, loss or prevention of the H-mode, divertor target hot spots and cessation of the plasma mode rotation at safety factor  $q=2$ . Locked modes are often followed by a disruption, particularly in lower-edge  $q$  discharges ( $q < 4$ ). Figure 1 shows parameter traces for a discharge in DIII-D<sup>1</sup> in which a modest  $n=1$  correction coil current ( $I_{n=1}$ ) partially cancels intrinsic error fields and prevents a locked mode; slowly increasing the coil current after 2000 msec increases the  $n=1$  error field re-

sulting in a locked mode at 3200 msec followed by a disruption.<sup>1</sup> Without the optimum correction coil, a locked mode occurs much earlier because of intrinsic, uncorrected error fields.

Experiments on COMPASS-C<sup>2</sup> and DIII-D show that careful design and coil alignment and/or correction of static field errors can allow routine operation in a wider stable parameter space without locked modes and subsequent disruptions.<sup>1,2</sup> A question for future devices such as International Thermonuclear Experimental Reactor (ITER)<sup>7</sup> is what level of resonant, low  $m$ ,  $n=1$  error field is tolerable for avoiding locked modes?

In this paper, sources of static error fields, particularly in COMPASS-C and DIII-D, are discussed in Sec. II. The experimental effect of varying the error field on locked mode instability is given in Sec. III. Comparison of nonlinear tearing stability theory in a rotating plasma with experiment is presented in Sec. IV. Extrapolation of the existing theory and experiments to the large ITER device is made in Sec. V. Conclusions are given in Sec. VI.

## II. SOURCES AND CORRECTION OF TOKAMAK ERROR FIELDS

The term "error field" is used for the toroidally non-axisymmetric fields resulting from (i) "as-designed" poloidal or toroidal field coil irregularities, i.e., from coil current feeds, turn-to-turn jogs, layer-to-layer transitions, etc.; (ii) "as-built" coils, i.e., coils fabricated with shape variations from as-designed or mounted with shifts and/or tilts from the nominal as-designed location. Error fields can also arise

\*Paper 616, Bull. Am. Phys. Soc. **36**, 2402 (1991).

<sup>†</sup>Invited speaker.

<sup>a)</sup>Also at Culham Laboratory, UKAEA/Euratom Fusion Association, Abingdon, England.

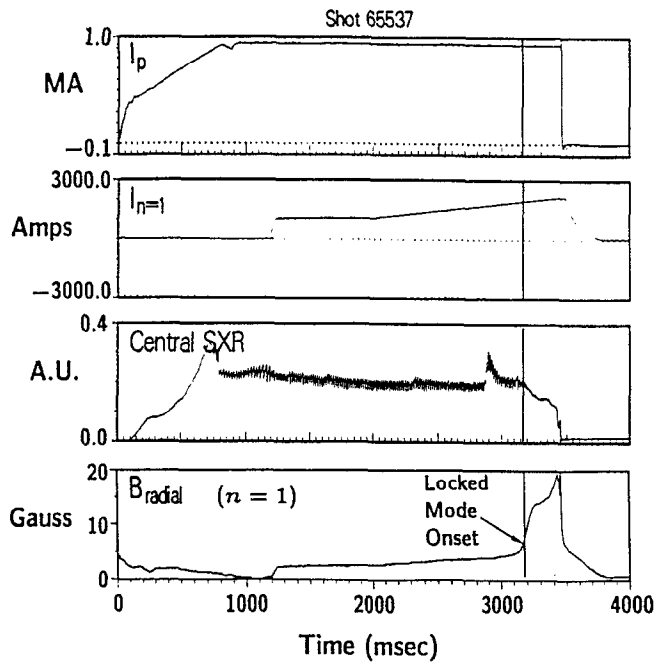


FIG. 1. Parameter traces for a DIII-D discharge in which a modest, optimum  $n=1$  correction coil current prevents a locked mode and then a nonoptimum, excessive current induces a locked mode: plasma current  $I_p$ ,  $n=1$  coil current  $I_{n=1}$ , central SXR,  $n=1$  radial field  $B_{\text{radial}}$  at the outboard midplane.

from magnetic material (shielding boxes, beams, etc.) or eddy currents in the vacuum vessel and/or support structures.

### A. Error fields in COMPASS-C

Careful design and magnetic alignment of the poloidal field coils in the small COMPASS-C tokamak (major radius  $R_0 = 0.557$  m) yield a device with very low field errors.<sup>8</sup> The COMPASS-C coils are aligned to  $\pm 0.5$  mm of concentricity with the toroidal field. The resulting relative, helical radial  $m=2$ ,  $n=1$  error field at minor radius  $a = 0.196$  m is  $B_{r21}/B_T|_a \approx 1 \times 10^{-5}$ , where  $B_T$  is the toroidal field. (The total  $B_{r1}/B_T$  from all  $m$  modes, both left and right handed is  $\lesssim 5 \times 10^{-5}$ .)

To produce static error fields, the resonant magnetic perturbation (RMP) winding is used. This consists of a selected set of up to ten one-turn bars distributed poloidally in each of the four toroidal quadrants, with appropriate poloidal segments also available. Many possible combinations can be made to produce different perturbing error fields. The example shown in the top view of Fig. 2 is a connection that produces a nearly pure, resonant  $m=2$ ,  $n=1$  helical mode.

### B. Error fields in DIII-D

Careful measurements of DIII-D error fields indicate that the dominant error field is an  $m \approx 2$ ,  $n=1$  error field that arises from nonconcentric outer poloidal field (F) coils, which produce the vertical field.<sup>9</sup> Typically, the intrinsic relative error field from the F-coil currents for a single-null divertor (SND) discharge with  $q$  at the 95%

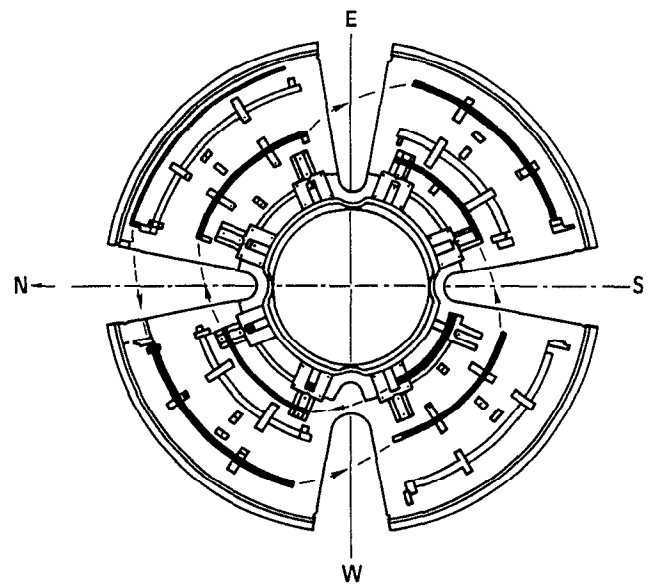


FIG. 2. Top view of COMPASS-C showing some of the RMP windings (dark bars) that produce a predominantly  $m=2$ ,  $n=1$  static error field. (Many other windings are possible.)

flux surface of  $q_{95} = 3.6$  in DIII-D is  $B_{r21}/B_T|_a \approx 1.7 \times 10^{-4}$  with  $a = 0.68$  m.

To partially cancel, or increase, the intrinsic  $n=1$  error fields, the “ $n=1$  coil” is used on DIII-D.<sup>1</sup> The  $n=1$  coil is a circular, 56-turn coil placed nonconcentrically on top of DIII-D as shown in Fig. 3; also shown are the outer F coils, F7A, F6A, F6B, F7B, which produce most of the error field as a result of nonconcentricity with the toroidal field. The  $n=1$  coil makes predominantly  $n=1$ ,  $m=1$  and 2 components. With the appropriate current, the net  $m=2$ ,  $n=1$  error field can be substantially reduced or increased. The  $n=1$  coil is now routinely used in DIII-D to reduce error fields; the coil current is controlled by a feedback algorithm that depends linearly on the currents in the F coils F7A, F6A, and F6B based on the measured error field

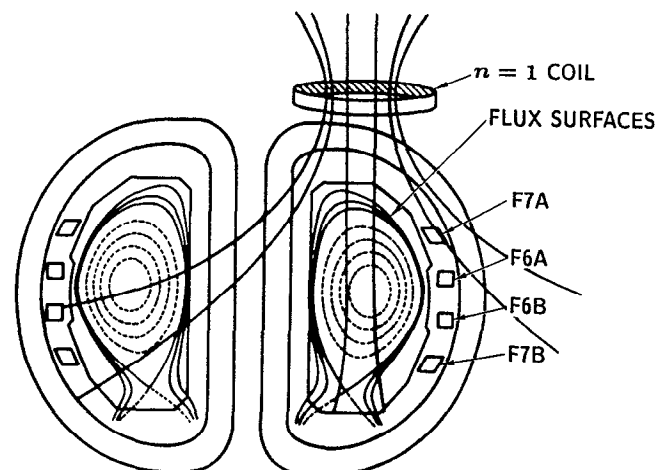


FIG. 3. Location of DIII-D  $n=1$  coil that is used to partially cancel intrinsic  $n=1$  error fields or to increase them.

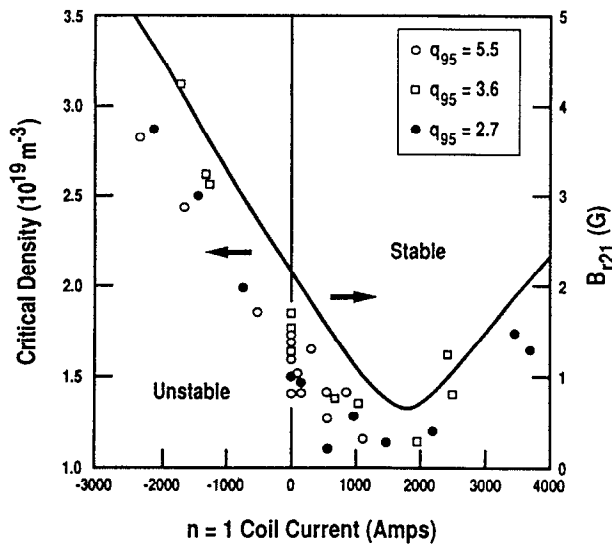


FIG. 4. Critical low density in DIII-D for locked modes and the  $m=2$ ,  $n=1$  error field versus  $n=1$  coil current; for zero current, the error field is from intrinsic F-coil irregularities. Discharges are of plasma current 0.95 MA, single-null divertor, Ohmically heated with  $B_T = 1.0$  T for  $q_{95} = 2.7$ ,  $B_T = 1.3$  T for  $q_{95} = 3.6$  and  $B_T = 2.0$  T for  $q_{95} = 5.5$ .

from these coils.<sup>9</sup> To minimize the  $m=2$ ,  $n=1$  error field, the current in the  $n=1$  coil is automatically adjusted to compensate for changes in plasma current, pressure, discharge shape, etc. A better-matched correction coil for DIII-D, the “C coil,” is designed, which will nearly eliminate a broader  $m$  spectrum of error fields, including the  $m=3$ ,  $n=1$  mode which is little affected by the  $n=1$  coil.<sup>10</sup>

### III. LOW-DENSITY LOCKED MODES DRIVEN NONLINEARLY UNSTABLE BY $m=2$ , $n=1$ ERROR FIELD

Locked modes can occur at either low or high density, at low  $q$ , at high beta, when large sawtooth crashes occur or when bursts of impurities enter a discharge. Low-density locked modes in COMPASS-C and DIII-D occur at a critical density that depends on the magnitude of the error field. Reducing the density  $\bar{n}$  at fixed  $B_{r21}$ , or increasing  $B_{r21}$  at fixed  $\bar{n}$ , leads to a locked mode under similar conditions.<sup>1,2</sup> Low-density, Ohmic target plasmas without locked modes are important for the supershot S mode<sup>11</sup> [Tokamak Fusion Test Reactor (TFTR)], the hot-ion H mode<sup>12</sup> (DIII-D), the VH mode<sup>13</sup> (DIII-D), and for rf current drive experiments. Experimentally, reducing the  $m=2$ ,  $n=1$  error field allows lower-density operation without locked modes and disruptions.

In COMPASS-C with very low intrinsic error fields ( $B_{r21}/B_T|_a \approx 1 \times 10^{-5}$ ), locked modes are not observed at low density unless error fields are deliberately produced by the RMP winding.

In DIII-D, reducing the intrinsic  $m=2$ ,  $n=1$  error field by use of the  $n=1$  coil allows stable operation at lower densities without locked modes and disruptions; the converse is also true, as with larger error fields, the stable parameter space is reduced. This is shown in Fig. 4, where

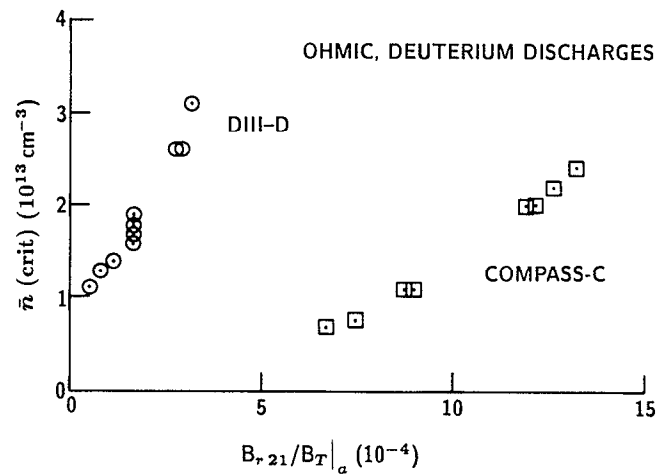


FIG. 5. Critical density for locked mode to occur in COMPASS-C, DIII-D versus relative, helical  $m=2$ ,  $n=1$  radial error field. Ohmic, deuterium discharges of similar aspect ratio, toroidal field, and  $q$ .

the critical low density for locked modes and the magnitude of the  $m=2$ ,  $n=1$  error field are plotted versus  $n=1$  coil current; for zero current the error field is from intrinsic F-coil irregularities and all discharges are 0.95 MA, Ohmic, deuterium, SND with  $B_T = 1.0$  T for  $q_{95} = 2.7$ ,  $B_T = 1.3$  T for  $q_{95} = 3.6$ , and  $B_T = 2.0$  T for  $q_{95} = 5.5$ . The stability is nonlinear in that, for small perturbations, discharges are stable and, for larger error fields, locked modes occur (which are often followed by disruptions at lower-edge  $q$ ). Typically on DIII-D, lower- $q$  plasmas are more sensitive to mode locking by error fields. The data shown in Fig. 4 for the lowest  $q_{95}$  of 2.7 are from a separate run-day than the others and atypically low in critical density. Wall conditions may subtly change profiles and stability.

The behavior of low critical density versus error field in COMPASS-C is similar, as shown in Fig. 5, where the “pure” 2, 1 RMP winding is used to make error field,<sup>2,14</sup> the DIII-D data for the  $q_{95} = 3.6$  case are also plotted. In these Ohmic, deuterium discharges with  $q$  at the edge of about 3.5 in each device, the small COMPASS-C ( $R_0 = 0.557$  m) is much more robust to error fields than the medium-sized DIII-D ( $R_0 = 1.67$  m), i.e., a much larger relative  $m=2$ ,  $n=1$  error field is needed to have a locked mode. The parameters for data from discharges plotted in Fig. 5 are given in Table I for comparison. The smaller COMPASS-C has much faster Mirnov activity of fre-

TABLE I. Comparison of COMPASS-C and DIII-D discharges of Fig. 5 (Ohmic, deuterium,  $a/R_0 \approx 1/3$ ).

	COMPASS-C	DIII-D
$R_0$ (m)	0.56	1.67
$B_T$ (T)	1.1	1.3
$f$ (kHz)	13	1.6
(Mirnov)		
Configuration	Limited, circular	Single-null divertor of elongation 1.6
	with $q_L = 3.5$	with $q_{95} = 3.6$

quency  $f=13$  kHz than the medium-sized DIII-D with  $f=1.6$  kHz (before locked modes occur and the Mirnov activity disappears).

#### IV. COMPARISON OF ERROR FIELD/LOCKING EXPERIMENTS WITH THEORY

In general, the tokamak plasma has a toroidal fluid rotation as indicated by Mirnov activity or by charge exchange spectroscopy measurements. (The plasma fluid rotation and mode rotations are not necessarily the same.) To this rotating, conducting fluid is applied a static  $n \neq 0$  error field. Nave and Wesson have considered the mode locking as an interaction of rotating tearing modes with resistive walls in which penetration of the rotating mode into the wall slows it, and for sufficiently large modes, essentially causes the rotation to cease, with the static error field only determining the locking location.<sup>15</sup>

Fitzpatrick and Hender have theoretically examined the penetration of a static helical magnetic perturbation into a rotating tokamak plasma.<sup>16</sup> In the linear regime for typical tokamak plasmas, the low  $m, n=1$  error fields and resulting islands are predicted to be suppressed by a large factor by the rotating plasma. In the nonlinear regime, a fairly sharp threshold is predicted for the magnitude of the applied static perturbation that can penetrate the rotating plasma and drive a locked island. The resulting islands can be substantially enhanced by the plasma response to the error field.<sup>17</sup>

The nonlinear tearing theory of the interaction of static resonant magnetic perturbations with the rotating plasma predicts a critical relative radial, helical error field at  $r=a$  of<sup>16</sup>

$$\frac{B_{rnl}}{B_T} \Big|_a \approx 6.7 [g^2] \left[ \left( \frac{r_s}{a} \right)^{2-m} \left( \frac{q^2 r_s}{m^4 R_0} \right)^{1/3} \left( \frac{-\Delta'_0 r_s}{S_B} \right)^{1/3} \right] \times [(f\tau_H)^{4/3}], \quad (1)$$

where the  $m, n$  mode is resonant at  $q=m/n$  at radius  $r_s$ , the term in the first bracket is a weak function of viscosity of  $\mathcal{O}(1)$ ,<sup>14,16</sup> the term in the second bracket is a function of the current profile and the mode [ $-\Delta'_0 r_s$  is the usual dimensionless tearing parameter and  $S_B = (rdq/dr/q^2)_r$  is a shear parameter], and the term in the third bracket is a strong function of the toroidal plasma rotation frequency at  $r = r_s$  and the Alfvén time  $\tau_H \equiv R_0 (\mu_0 \bar{n} m_i)^{1/2} / B_T$ , where  $m_i$  is the ion mass.

The dominant term in Eq. (1) predicts that

$$B_{r21}/B_T \Big|_a \sim (fR/B_T)^{4/3} \bar{n}^{-2/3}. \quad (2)$$

Taking measurements or reasonable estimates for the parameters in Eq. (1), the experimental results in COMPASS-C and DIII-D (as shown in Fig. 5) are in good agreement with the theory both in absolute value and relative value from device to device. The larger, more slowly rotating plasma of DIII-D compared to COMPASS-C ( $f \approx 1.6$  kHz versus 13 kHz) is more sensitive to error fields penetrating the plasma and nonlinearly inducing a locked mode. Note that the COMPASS-C data are close to the

predicted dependence  $B_{r21}/B_T \Big|_a \sim \bar{n}^{2/3}$  while the DIII-D data are a poorer fit. This difference can be explained by the use of a “pure”  $m=2, n=1$  perturbation in COMPASS-C, while in DIII-D the  $n=1$  coil can reduce the  $m=2, n=1$  error field or increase it but has little effect on reducing the  $m=3, n=1$  component, which may thus explain the offset from the theory.

#### V. CRITICAL ERROR FIELD PREDICTED FOR ITER

Considering only Ohmically heated, deuterium discharges of similar edge  $q$  and aspect ratio, one expects that current density profiles will be similar from device to device.<sup>18</sup> Thus the second bracket in Eq. (1) is assumed to be similar. The Ohmically heated discharges considered here have Mirnov activity at a frequency  $f$  about that of the electron drift frequency  $f_{De}$  where

$$f \approx f_{De} \approx \kappa_B T_{e0} / e B_T a^2, \quad (3)$$

with  $\kappa_B$  the Boltzmann constant and  $T_{e0}$  the central electron temperature.<sup>19</sup> For COMPASS-C,  $T_{e0} \approx 600$  eV,  $B_T = 1.1$  T,  $a=0.18$  m, and  $f_{De} \approx 15$  kHz compared to measured  $f \approx 13$  kHz. For DIII-D,  $T_{e0} \approx 920$  eV,  $B_T = 1.3$  T,  $a=0.64$  m, and  $f_{De} \approx 1.7$  kHz compared to measured  $f \approx 1.6$  kHz.

The scaling of the central electron temperature in an Ohmic discharge is obtained by balancing the Ohmic power input with the anomalous energy loss. For Pfeiffer-Waltz scaling of electron energy confinement time  $\tau_{Ee}$ ,<sup>20</sup> which was obtained by regression fitting of Ohmic data,

$$T_{e0} \sim \left( \frac{\tau_{Ee}}{\bar{n}} \right)^{2/5} \left( \frac{I_p}{\pi a^2} \right)^{4/5}, \quad (4)$$

$$\tau_{Ee} \sim \bar{n} a R_0^{3/2}, \quad (5)$$

and

$$f \approx f_{De} \sim R_0^{-9/5} B_T^{-1/5}, \quad (6)$$

for the same  $q$  ( $a^2 B_T / R_0 I_p$  is constant) and inverse aspect ratio ( $\epsilon = a/R_0$  is constant). Thus one expects that for Ohmically heated plasmas with plasma rotation frequency at  $q=2$  about the electron drift frequency, larger tokamak plasmas will rotate slower. The scaling given by Eq. (6) is quite good in comparing COMPASS-C to DIII-D; the simple scaling relation predicts a sevenfold faster rotation in COMPASS-C than DIII-D compared to the measured eight times faster frequency.

Now combining Eqs. (2) and (6) for scaling of the critical error field for locked modes and assuming that the equivalent density scales as<sup>21</sup>

$$\bar{n} \sim B_T / R_0, \quad (7)$$

one obtains for the scaling of the critical relative error field

$$B_{r21}/B_T \Big|_a \sim R_0^{-26/15} B_T^{-14/15}, \quad (8)$$

where we reiterate that current profiles, edge  $q$  and  $\epsilon$  are assumed to be the same in Ohmically heated deuterium discharges. Thus, particularly as  $B_T \sim R$  in most existing or planned tokamaks, there is a strong reduction with  $R_0$  in

TABLE II. Extrapolation of Ohmic, deuterium discharges at  $q_{95} = 3.6$  from DIII-D to ITER.

	DIII-D	ITER
$R_0$ (m)	1.67	6.0
$B_T$ (T)	1.3	4.9
$\bar{n}R_0/B_T$ at $2 \times 10^{13} \text{ cm}^{-3}$	2.6	2.5
$f \approx f_{De}$ (kHz)	1.6	0.17
$g^2$	(measured) 3.1	(predicted) 5.9
$B_{r21}/B_T _{a \text{ crit}} \sim g^2 \left(\frac{fR}{B_T}\right)^{4/3} \bar{n}^{2/3}$	$1.7 \times 10^{-4}$ (measured)	$2 \times 10^{-5}$ (predicted)

the predicted critical error field for locked modes. [Differences in elongation can readily be taken into account in  $q$  and Eqs. (4)–(6).]

The critical  $m=2$ ,  $n=1$  error field in DIII-D is scaled up to ITER size for a fixed density  $\bar{n} = 2 \times 10^{13} \text{ cm}^{-3}$  (nearly constant  $\bar{n}R_0/B_T$ ) at  $q_{95} = 3.6$  assuming similar current profiles, and explicitly evaluating the weak viscous function  $g^2$ ; differences in aspect ratio and elongation have also been taken into account. The comparison is shown in Table II. The larger ITER device is predicted to have a much slower plasma rotation frequency and, as a result, is predicted to be more sensitive to error fields nonlinearly inducing a locked mode. The critical  $m=2$ ,  $n=1$  relative error field is predicted to be only  $B_{r21}/B_T|_a \approx 2 \times 10^{-5}$ . (This is comparable to a level obtained on COMPASS-C by careful design and alignment.) With the same coil configuration as in DIII-D, a shift or tilt of any single outer ITER poloidal field coil of  $\pm 0.6$  cm would make a critical error field to produce a locked mode. Of course, the ITER coil configuration, when finally designed, will be different and such error field computations will have to be done for that case.

Higher density in ITER would increase the Alfvén time making the critical error field larger, but too high of a density (approaching the density limit) makes a steeper, more unstable current profile lowering the critical error field. Faster plasma rotation is predicted to make the ITER discharge less sensitive to a locked mode induced by error fields. Co-injected neutral beams in the current ramp-up of DIII-D are, indeed, sometimes experimentally effective in avoiding locked modes. Any means to increase the rotation frequency would obviate the sensitivity to error fields and increase allowable tolerances on ITER coil construction.

## VI. CONCLUSIONS

At lower  $q$  ( $\lesssim 4$ ), locked modes generally cause disruptions and so must be avoided. Typically, most locked-mode discharges with  $q < 4$  in DIII-D disrupt as a result of a combination of large islands, poor confinement, and cessation of any plasma wall stabilization. Reducing the low  $m$ ,  $n=1$  error fields increases the locked mode-free operating parameter space and helps avoid disruptions. Experiments are in agreement with theory in that larger, more

slowly rotating tokamak plasmas are more sensitive to error fields nonlinearly inducing locked modes.

Extrapolating from existing devices to the ITER plasma, the predicted relative critical error field for locked modes is quite small,  $B_{r21}/B_T|_a \approx 2 \times 10^{-5}$ . If locking occurs in ITER with error fields of this level, the resulting magnetic islands could be quite small. However, experimental experience shows that the locked plasma can respond to the error field in such a way as to amplify the islands, and several theoretical models predict island growth.<sup>22,23</sup> Experimentally, the island grows with time until a disruption occurs, particularly for edge  $q < 4$ . Further, mode rotation at  $q=2$ , for example, ceases as the mode locks to the static error field and any wall stabilization of instabilities is lost.

A means to increase the plasma rotation frequency (co-injected beams in DIII-D, for example, increase rotation) would lessen the sensitivity of a large plasma to error fields and reduce difficulties with very precise design and coil alignment or the requirement for an error field correction coil.

## ACKNOWLEDGMENTS

We would like to thank R. D. Stambaugh for arranging this collaboration. One of us (R.J.L.) thanks the COMPASS-C team for their hospitality during his visits.

This work was supported, in part, by the U.S. Department of Energy under Contract No. DE-AC03-89ER51114.

- <sup>1</sup>J. T. Scoville, R. J. La Haye, A. G. Kellman, T. S. Osborne, R. D. Stambaugh, E. J. Strait, and T. S. Taylor, Nucl. Fusion **31**, 875 (1991).
- <sup>2</sup>A. W. Morris, R. Fitzpatrick, T. C. Hender, T. N. Todd, the COMPASS Team, R. J. La Haye, and J. T. Scoville, in *Proceedings of the 18th European Conference on Controlled Fusion and Plasma Physics*, Berlin (EPS, Petit-Lancy, Switzerland, 1991), Vol. 15C, Part II, p. 61.
- <sup>3</sup>The ASDEX Team, Nucl. Fusion **25**, 1959 (1989).
- <sup>4</sup>J. Snipes, D. J. Campbell, P. S. Haynes, T. C. Hender, M. Hugon, P. J. Lomas, N. J. Lopes Cardozo, M. F. F. Nave, and F. C. Schüller, Nucl. Fusion **28**, 1275 (1988).
- <sup>5</sup>H. Ninomiya, K. Itami, Y. Neyatani, O. Naito, and R. Yoshino, Nucl. Fusion **28**, 1275 (1988).
- <sup>6</sup>V. V. Volkov, A. A. Gurov, N. V. Ivanov, A. M. Kakurin, and D. A. Martynov, Sov. J. Plasma Phys. **17**, 7 (1991).
- <sup>7</sup>J. P. Christiansen, J. G. Cordey, and K. Thomsen, Nucl. Fusion **30**, 1183 (1990).
- <sup>8</sup>R. J. Crossland, R. J. Hayward, T. N. Todd, P. S. Haynes, J. W. Hill, A. W. Morris, P. Nicholson, and R. A. Crook, in *Proceedings of the 16th Annual Symposium on Fusion Technology*, London, 1990 (Pergamon, New York, in press).
- <sup>9</sup>R. J. La Haye and J. T. Scoville, Rev. Sci. Instrum. **62**, 2146 (1991).
- <sup>10</sup>J. T. Scoville and R. J. La Haye, in *Proceedings of the 14th IEEE/NPSS Symposium on Fusion Engineering*, San Diego, 1991 (IEEE, New York, 1992), Vol. 2, p. 1144.
- <sup>11</sup>R. J. Fonck, R. Howell, K. Jaehnle, L. Roquemore, G. Schilling, S. Scott, M. C. Zarnstorff, C. Bush, R. Goldston, H. Hsuan, D. Johnson, A. Ramsey, J. Schivell, and H. Towner, Phys. Rev. Lett. **53**, 520 (1989).
- <sup>12</sup>K. H. Burrell, R. J. Groebner, T. S. Kurki-Suonio, T. N. Carlstrom, R. R. Dominguez, P. Gohil, R. A. Jong, H. Matsumoto, J. M. Lohr, T. W. Petrie, G. D. Porter, G. T. Sager, H. St. John, D. P. Schissel, S. M. Wolfe, and the DIII-D Research Group, *Plasma Physics and Controlled Nuclear Fusion Research*, Washington, DC, 1990 (IAEA, Vienna, 1991), p. 123.
- <sup>13</sup>G. L. Jackson, J. Winter, T. S. Taylor, K. H. Burrell, J. C. DeBoo, C. M. Greenfield, R. J. Groebner, T. Hodapp, K. Holtrop, T. W. Petrie, J.

- Phillips, D. P. Schissel, E. J. Strait, and A. D. Turnbull, *Phys. Rev. Lett.* **67**, 3098 (1991).
- <sup>14</sup>A. W. Morris, P. G. Carolan, R. Fitzpatrick, T. C. Hender, and T. N. Todd, submitted to *Phys. Fluids B*.
- <sup>15</sup>M. F. F. Nave and J. A. Wesson, in *Proceedings of the 14th European Conference on Controlled Fusion and Plasma Physics*, Madrid (EPS, Petit-Lancy, Switzerland, 1987), Vol. 3, p. 1103.
- <sup>16</sup>R. Fitzpatrick and T. C. Hender, *Phys. Fluids B* **3**, 644 (1991).
- <sup>17</sup>A. Reiman and D. Monticello, *Phys. Fluids B* **3**, 2230 (1991).
- <sup>18</sup>B. B. Kadomtsev, *Sov. J. Plasma Phys.* **13**, 443 (1987).
- <sup>19</sup>W. M. Manheimer, *An Introduction to Trapped-Particle Instability in Tokamaks* (Technical Information Center, Energy Research and Development Administration, Oak Ridge, TN, 1977), p. 17–20.
- <sup>20</sup>W. W. Pfeiffer and R. E. Waltz, *Nucl. Fusion* **19**, 51 (1979).
- <sup>21</sup>M. Greenwald, J. L. Terry, S. M. Wolfe, S. Ejima, M. G. Bell, S. M. Kaye, and G. H. Neilson, *Nucl. Fusion* **28**, 2199 (1988).
- <sup>22</sup>J. A. Wesson, A. Sykes, and M. F. Turner, in *Proceedings of the 10th International Conference on Plasma Physics and Controlled Nuclear Fusion Research*, London (IAEA, Vienna, 1985), Vol. 2, p. 23.
- <sup>23</sup>T. H. Jensen and W. B. Thompson, *Phys. Fluids* **30**, 3502 (1987).